

$\cong 3$. As in NiPcI, resonance Raman spectra for the $x \cong 3$ phase imply that the iodine is in the form of the chainlike triiodide. The $\theta = 0^\circ$ structure (with the appropriate a and b lattice constants) could readily accommodate the increased iodine content of the $x \cong 3$ phase, and this seems to be a likely structure for this material. In contrast, the recently isolated PF_6^- and BF_4^- salts of $\text{NiPc}^{\text{p}+4\text{c}}$ would require $\theta > 40^\circ$, on the assumption that the tetragonal lattice is retained. PF_6^- or BF_4^- situated at $(a/2, a/2, c/4)$ would require a larger volume than an iodine at the same site, and this could be most easily accomplished by a small, increased rotation of the macrocyclic rings. Of course, the Madelung energy for these materials could be significantly different from the iodinated crystal, largely depending on the degree of ordering in the

counterion stacks, and this could require a substantially different structure to ensure stability. Currently, Madelung energy calculations for $\text{NiPc}(\text{PF}_6)_{0.36}$ and $\text{NiPc}(\text{BF}_4)_{0.34}$ are in progress.

Acknowledgment is made to the donors of the Petroleum Research Fund, administered by the American Chemical Society, for partial support of this research. The Academic Computing Center at the University of Rhode Island is also acknowledged for the generous allotment of computer time. I also thank Professor Brian Hoffman for helpful discussions and the reviewer for the suggestion to include case 4.

Registry No. NiPcI, 66625-96-5.

Contribution from the Departments of Chemistry, Queens College, City University of New York, Flushing, New York 11367, and University of Connecticut, Storrs, Connecticut 06268

Spectral and Photophysical Properties of Ruthenium(II) 2-(Phenylazo)pyridine Complexes

STEVEN WOLFGANG,[†] THOMAS C. STREKAS,*[†] HARRY D. GAFNEY,*[†] RONALD A. KRAUSE,[‡] and KIRSTEN KRAUSE[‡]

Received November 10, 1983

Resonance Raman and emission spectra are reported for a series of complexes $\text{Ru}(\text{azpy})_2\text{L}_2^{n+}$ where azpy represents 2-(phenylazo)pyridine and L various monodentate ligands or a bidentate ligand. The resonance Raman spectra reveal a relatively localized MLCT excited state with large distortions of the azo $\text{N}=\text{N}$ bond. Emission maxima for the luminescent complexes are significantly red shifted relative to those for other Ru(II) diimine complexes. These data along with previously measured electrochemical data suggest an energy level ordering in which the luminescent LMCT state is an exergonic oxidant and endergonic reductant. Quenching by a series of related oxidative and reductive quenchers is consistent with the calculated energetics of the photoinduced redox processes.

Introduction

The correlation between excited-state redox potentials and luminescence spectra has led to extensive investigations of Ru(II) polypyridine complexes.¹ During the last decade, a variety of substituted 1,10-phenanthroline (phen) and 2,2'-bipyridine (bpy) complexes have been prepared as a means to modify and tune the complexes' photophysical and photo-redox properties.²⁻⁴ In most instances, however, the perturbation introduced by the substituent is relatively small and the photoinduced properties of the substituted complexes remain essentially those of the parent analogue. Substantial modification of the excited-state properties apparently demands significant change in the bidentate, π -accepting ligands.

Recently, two of us described the preparation of a series of new Ru(II) complexes of the general formula $\text{Ru}(\text{azpy})_2\text{L}_2^{n+}$ where azpy represents 2-(phenylazo)pyridine.⁵ L represents a series of mono- and bidentate ligands of differing σ -donor and π -acid capabilities. The visible spectra of these complexes are dominated by intense visible transitions where the transition energy and an IR frequency assigned to the azo $\text{N}=\text{N}$ stretch are functions of the π acidity of the coligands L. Our interest, however, was spurred by the luminescence and electrochemical behavior of these azpy complexes. When compared to those properties of the well-studied $\text{Ru}(\text{bpy})_3^{2+}$,^{6,7} the luminescence of the parent analogue, $\text{Ru}(\text{azpy})_3^{2+}$, occurs at a lower energy and the complex has a larger oxidation potential, but a smaller reduction potential. This suggests an unusual energy level ordering in which the energy required to oxidize the ground

state of $\text{Ru}(\text{azpy})_3^{2+}$ exceeds the energy of the luminescent excited state. This inversion of the energy levels is quite different from that found with the polypyridine complexes, where the energy of the luminescent state generally exceeds that of the thermal redox steps and the excited state can act as an exergonic reductant or oxidant.² For the azpy complexes, however, the data suggest that reductive quenching of $\text{Ru}(\text{azpy})_3^{2+}$ is exergonic whereas oxidative quenching of the complex is endergonic. For oxidative quenching to occur, the reduction potential of the quencher plus the excited-state energy must exceed the thermal oxidation potential of $\text{Ru}(\text{azpy})_3^{2+}$. Consequently, reductive quenching by a quencher of known oxidation potential is also a means of bracketing the thermal oxidation potentials of the complexes, which are presently known only as lower limits.

To test these ideas based on luminescence-electrochemical energy changes, we have examined the photophysical properties and photoredox behavior of these $\text{Ru}(\text{azpy})_2\text{L}_2^{n+}$ complexes. Resonance Raman spectra of the complexes confirm the MLCT character of the visible absorptions and suggest an excited-state configurations in which a significant portion of

- (1) Kalyanasundaram, K. *Coord. Chem. Rev.* **1982**, *46*, 161 and references therein.
- (2) Lin, C. T.; Botcher, W.; Chou, M.; Creutz, C.; Sutin, N. *J. Am. Chem. Soc.* **1976**, *98*, 6536.
- (3) Berler, P.; von Zelewsky, A. *Helv. Chim. Acta* **1980**, *63*, 1675.
- (4) Fabian, R. H.; Klassen, D. M.; Sonntag, R. W. *Inorg. Chem.* **1980**, *19*, 1977.
- (5) Krause, R.; Krause, K. *Inorg. Chem.* **1982**, *21*, 1714.
- (6) Paris, J. P.; Brandt, W. W. *J. Am. Chem. Soc.* **1959**, *81*, 5001.
- (7) Tokel-Takvoryan, N. E.; Hemingway, R. E.; Bard, A. J. *J. Am. Chem. Soc.* **1973**, *95*, 6582.

[†]City University of New York.

[‡]University of Connecticut.

the transferred charge is localized on the azo function. Photon counting following laser excitation of room-temperature fluid solutions and solid samples of the complexes reveals low-intensity near-IR emissions from a number of the complexes. Ru(azpy)₃²⁺ and Ru(azpy)₂(btz)₂²⁺ (btz denotes 4,4'-bithiazole) appear to crystallize as two isomeric forms since emission spectra of solid samples of the complexes show two maxima but a single emission maximum when these samples are dissolved in fluid solution. Quenching studies with related pairs of oxidative and reductive quenchers are consistent with the calculated excited-state potentials and an excited state that is an exergonic oxidant and endergonic reductant.

Experimental Section

Materials. The Ru(azpy)₂Lⁿ⁺ complexes, where L denotes 2-(phenylazo)pyridine (azpy), 2,2'-bipyridine (bpy), 4,4'-bithiazole (btz), ethylenediamine (en), acetylacetonate (acac) thiourea (tu), (CN⁻)₂, and (NO₂)₂ were prepared by previously described procedures⁵ and isolated as either neutral complexes or perchlorate or hexafluorophosphate salts. Ceric ammonium sulfate was standardized with As₂O₃ according to the procedure of Skoog and West.⁸ All other chemicals were reagent grade, and solutions were prepared with spectral grade solvents or with water distilled in a Corning distillation apparatus. Solutions were deaerated by bubbling with prepurified N₂ (Linde).

Physical Measurements. Absorption and Emission Spectra. UV-visible spectra were recorded on either a Cary 11 or a Cary 14 spectrophotometer. At room temperature, these complexes are weak emitters and the spectral sensitivity of a Perkin-Elmer Hitachi MPF-2A emission spectrophotometer, although equipped with a Hamamatsu R818 red-sensitive photomultiplier, was not sufficient to reliably record the emission spectra. To obtain the emission spectra, solid samples or 10⁻⁵–10⁻⁴ M solutions of the complexes were placed in 1 mm i.d. capillary tubes and excited at 514.5 nm with an Ar laser. **Caution!** Solid samples of [Ru(azpy)₂(btz)](ClO₄)₂ spontaneously detonated when exposed to a focused 514.5-nm laser beam at a power of 30 mW. The emission from each complex was monitored at 90° to the excitation with a Raman spectrometer equipped with photon-counting detection. Freshly prepared 10⁻⁴ M stock solutions of the Ru(azpy)₃²⁺ complex containing different amounts of the quenchers were used for emission-quenching experiments.⁵ Aliquots of each solution were sealed in capillary tubes and excited at 514.5 nm, and the emission intensities were monitored at 830 nm. The emission intensity from the solution containing only the Ru(II) complex was measured periodically during the course of the quenching experiments to establish that alignment of the capillary tubes on the sample stage of the Raman spectrometer did not introduce a significant error in the quenching data. The emission intensity from solutions containing both donor and quencher were also measured as a function of time to establish that the laser excitation did not cause a net photochemical reaction.

Emission Lifetimes. Room-temperature luminescence lifetimes of the complexes in fluid solution were measured by previously described signal-averaging techniques.⁹ With the exception of Ru(azpy)₃²⁺, however, the emission decays for the other complexes, which are lower energy and lower intensity emitters, did not have a large enough signal to noise ratio to be considered reliable.

Resonance Raman Spectra. Spectra of chloroform or water solutions of the complexes were recorded with a previously described Raman spectrometer.¹⁰ Solutions of the complexes, typically 5 × 10⁻³ M, contained in capillary tubes were excited with an Ar laser line close to the absorption maximum, and the Raman scattering was monitored at 90° to the transverse excitation beam. Optical spectra of the solutions were recorded before and after the Raman experiments to check sample integrity.

Results and Discussion

Resonance Raman Spectra. When the complexes were excited close to the maximum of the visible absorption band, the resonance Raman spectra of the Ru(azpy)₂L₂ⁿ⁺ complexes consist of a series of bands in the 200–1650-cm⁻¹ region. For

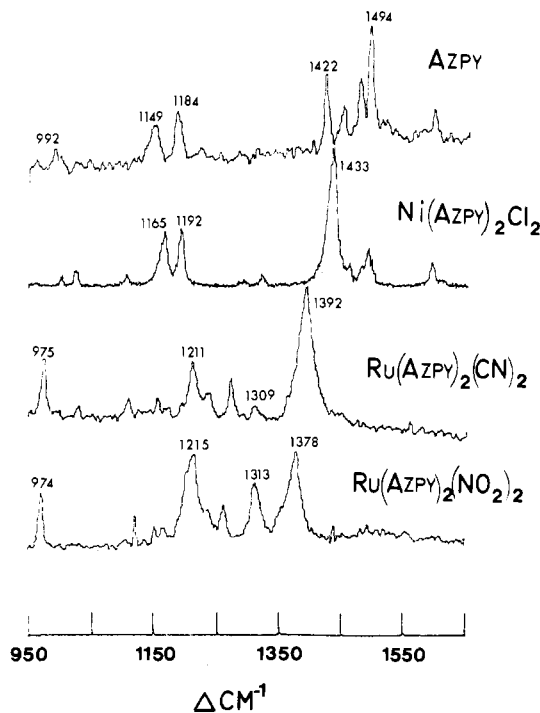


Figure 1. Raman spectra of azpy (457.9-nm excitation) and Ni(azpy)₂Cl₂ (457.9-nm excitation) and resonance Raman spectra of Ru(azpy)₂(CN)₂ (574.6-nm excitation) and Ru(azpy)₂(NO₂)₂ (514.5-nm excitation). Note the marked shift of band assigned as ν_{N=N} in the 1350–1424-cm⁻¹ region.

Table I. Raman Bands^a for Ru(azpy)₂Lⁿ⁺ Complexes Showing Greatest Enhancement

coligand (L)	Ph	no. 2	no. 3	N=N
2 CN ⁻	975	1211	1309	1392
2 NO ₂ ⁻	974	1215	1313	1378
btz	975, 991	1204	1315	1360, 1375 sh
bpy	976	1201	1317	1364
azpy	966, 975	1200	1317	1368, 1384 sh
en	980	1209	1316	1360
acac ⁻	981	1207	1313	1346
2 Br ⁻	978	1212	1311	1350
2 N ₃ ⁻	977	1216	1309	1338
2 Cl ⁻ , α ^b	977	1209	1311	1345
2 Cl ⁻ , β ^c	976	1209	1310	1337

^a Frequency in cm⁻¹. ^b α isomer. ^c β isomer.

all complexes, however, the most intense resonance enhancement occurs for a series of bands in the 950–1400-cm⁻¹ region, and typical spectra of this region are shown in Figure 1. Also included is a spectrum of Ni(azpy)₂Cl₂,¹¹ although this is most likely not a resonance Raman spectrum but a preresonance spectrum. Table I lists the frequencies of the four bands that show the most significant resonance enhancement for the Ru(azpy)₂L₂ⁿ⁺ complexes. With the exception of one band, which is discussed in detail below, the band frequencies vary <10 cm⁻¹ for the entire series of complexes. Because of this invariance and their commonality to all complexes, regardless of the other ligands, the vibrations are assigned to the azpy ligand. No bands attributable to any other source, except the solvent, occur in any of the resonance Raman spectra. The pronounced enhancement of these azpy vibrations when the intense visible absorption is excited confirms that the latter is an Ru(II) t₂ MLCT transition that terminates in an azpy π* orbital.

The assignment of all resonance Raman bands must await a normal-coordinate analysis, but several qualitative assign-

(8) Skoog, D. A.; West, D. M. "Fundamentals of Analytical Chemistry"; Holt, Rinehart and Winston: New York, 1963; p 452.
 (9) Wolfgang, S.; Gafney, H. D. *J. Phys. Chem.*, in press.
 (10) Valance, W. G.; Streckas, T. C. *J. Phys. Chem.* **1982**, *86*, 1804.

(11) Clark, R. J. H.; Stewart, B. *Struct. Bonding (Berlin)* **1979**, *36*, 1.

ments can be made. The frequencies listed in Table I show that, in contrast to the other bands, whose frequencies vary $<10\text{ cm}^{-1}$, the band found between $1337\text{ (L = 2 Cl}^-)$ and 1392 cm^{-1} (L = 2 CN^-) and at 1433 cm^{-1} for the Ni(II) complex, a weak π -back-bonding metal, is generally of highest relative intensity and shows significant frequency variation. Since the frequencies of this band correspond to those for the azo $\text{N}=\text{N}$ stretch in the IR spectra,^{5,12} the band is assigned to the azo $\text{N}=\text{N}$ stretch. Tsuboi's rule¹³ states that the largest enhancement in resonance Raman scattering is observed for the molecular coordinates that undergo the greatest distortion in the excited state. Since the band attributed to the azo $\text{N}=\text{N}$ stretch is the most intense, we can infer that the charge transferred from the Ru(II) t_2 orbitals resides in azpy anti-bonding π^* orbitals localized principally in the azo $\text{N}=\text{N}$ region of the ligand. In the excited state, therefore, the $\text{N}=\text{N}$ bond is highly distorted.

Other bands show significant resonance enhancement, with some variations from spectrum to spectrum. Bands near 980 , 1205 , and 1315 cm^{-1} consistently show intensity and in some spectra high relative intensity. These bands must be associated with bonds contiguous to the azo $\text{N}=\text{N}$ bond in the azpy ligand, including the C-N (pyridine) and N-C (phenyl) bonds. Also, the 980-cm^{-1} band is within the region expected for a phenyl ring breathing mode. This suggests that the phenyl ring system is an intimate part of the chromophore and is probably conjugated with the $\text{N}=\text{N}$ bonding system to some extent.

In contrast, vibrations assignable to the pyridyl substituent that is directly coordinated to the Ru(II) are very weak. In particular, pyridyl symmetric breathing modes, generally found in the $1000\text{--}1050\text{-cm}^{-1}$ region and typically among the most intense in the resonance Raman spectra of pyridine- and polypyridine-substituted metal complexes,¹⁴ are observed but are of extremely low intensity. Low-intensity bands above 1450 cm^{-1} , which are assignable to other pyridine ring modes, are also present.

The resonance Raman data suggest the following picture of the excited state of $\text{Ru}(\text{azpy})_2\text{L}_2^{n+}$. In general, the electron density in the excited state is centered on the π system, which includes the azo $\text{N}=\text{N}$ bond and the C-N bonds adjacent to it. Surprisingly, the pyridine moiety is only weakly involved in accepting the charge, whereas the phenyl ring, since it appears to be conjugated with the azo $\text{N}=\text{N}$ bond, is involved in accepting some of the charge.

Absorption and Emission Spectra. As mentioned above, the intense visible absorptions of these azpy complexes are assigned, assuming O_h microsymmetry, to Ru(II) t_2 to azpy π^* MLCT transitions. Excitation of these transitions induces near-IR emission from room-temperature ($22 \pm 1\text{ }^\circ\text{C}$) solid samples of $\text{Ru}(\text{azpy})_2\text{L}_2^{n+}$, where $\text{L} = \text{azpy, btz, bpy, en, acac}^-$, $(\text{NO}_2^-)_2$, $(\text{CN}^-)_2$, and tu , and weaker emissions from room-temperature fluid solutions of $\text{Ru}(\text{azpy})_3^{2+}$, $\text{Ru}(\text{azpy})_2(\text{btz})_2^{2+}$, $\text{Ru}(\text{azpy})_2(\text{bpy})_2^{2+}$, and $\text{Ru}(\text{azpy})_2(\text{CN})_2$. The unusual asymmetry of representative emission spectra shown in Figure 2 is due to the spectral sensitivity of the photomultiplier, which rapidly declines at 870 nm . As a result, all spectra truncate at 870 nm and, for many of the complexes, only lower limits of the actual emission maxima are listed in Table II. For those complexes that show measurable emission maxima, however, the emission energies parallel the MLCT absorption energies,⁵ and in accord with previous studies,¹⁵ the emissions are assigned to azpy $\pi^*\text{-Ru(II) } t_2$ transitions.

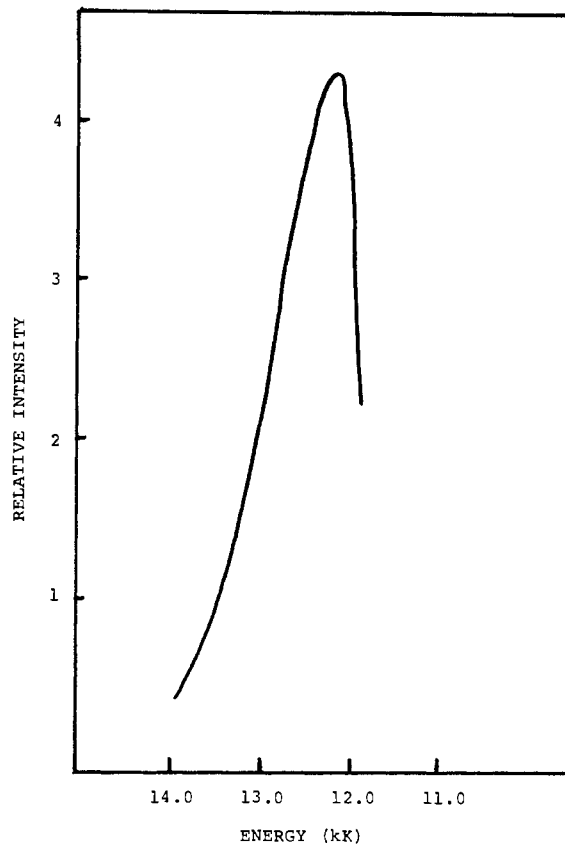


Figure 2. Emission spectrum of $\text{Ru}(\text{azpy})_3^{2+}$ in H_2O at room temperature ($22 \pm 1\text{ }^\circ\text{C}$), excited at 514.5 nm with an argon ion laser.

Table II. Emission Maxima and Redox Potentials of the $\text{Ru}(\text{azpy})_2\text{L}^{n+}$ Complexes

coligand	emission max, ^a nm	E, V^b	
		III \rightarrow II	II \rightarrow I
azpy	784, 846 (835)		0.30
btz	776, 833 (≥ 870)	2.0	-0.19
bpy	854 (≥ 870)		0.17
(CN) ₂	≥ 870		-0.24
acac	≥ 870	1.78	-0.14
en	≥ 870		-0.07
(NO_2) ₂	≥ 870		-0.22
(tu) ₂		1.38	-0.08
Br_2		1.43	-0.30
(N_3) ₂ ^c		1.2	-0.28
$\alpha\text{-Cl}_2$ ^c		1.45	
$\beta\text{-Cl}_2$ ^c		1.39	

^a Values in parentheses are emission maxima from room-temperature acetone solutions of the complexes. ^b Reduction potentials relative to the standard hydrogen electrode. ^c Refer to the α and β isomers.

As indicated in Table II, room-temperature solid samples of $[\text{Ru}(\text{azpy})_3](\text{PF}_6)_2$ and $[\text{Ru}(\text{azpy})_2(\text{btz})](\text{PF}_6)_2$ show two emission maxima. Although the emission maxima of the btz complex differ from that found at 77 K ,⁵ the difference is attributed to the spectral sensitivities of the detectors and the 755- and 822-nm transitions at 77 K correspond, respectively, to the 776- and 833-nm transitions at room temperature. Maxima at 784 and 846 nm occur in the room-temperature emission spectra of solid samples of $[\text{Ru}(\text{azpy})_3](\text{PF}_6)_2$, whereas a single maximum at 764 nm was found in the low-temperature spectra.⁵ Since the difference in energy between the 784- and 764-nm transitions, 334 cm^{-1} , is similar to the shift of the higher energy $[\text{Ru}(\text{azpy})_2(\text{btz})](\text{PF}_6)_2$ transition, 358 cm^{-1} , these maxima are assigned to the same transition, and the absence of a second peak in the low-temperature spectra is attributed to differences in the spectral sensitivities

(12) Krause, R.; Krause, K. *Inorg. Chem.* **1980**, *19*, 2600.

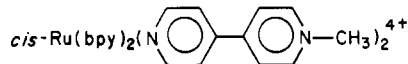
(13) Nishimura, Y.; Hirakawa, A. Y.; Tsuboi, M. *Adv. Infrared Raman Spectrosc.* **1978**, *5*.

(14) Unpublished observation.

(15) Klassen, D. M.; Crosby, G. A. *J. Chem. Phys.* **1968**, *48*, 1853.

of the detector rather than a fundamental molecular change.

The two emissions from either complex are not due to a photoinduced reaction since the relative intensities are independent of exposure time. Previously, the two emissions from solid samples of the btz complex at 77 K were attributed to transitions originating in azpy π^* and btz π^* orbitals.⁵ However, the assignment appears unlikely in view of the data gathered here. Meyer and co-workers¹⁶ point out the reproducibility of the multiple emissions from



under a variety of experimental conditions. Comparing spectra of several solid samples of either $[\text{Ru}(\text{azpy})_3](\text{PF}_6)_2$ or $[\text{Ru}(\text{azpy})_2(\text{btz})](\text{ClO}_4)_2$ shows that the emission maxima occur at the same wavelength, but the relative intensities of the two emissions are not reproducible. Even samples of each complex taken from the same preparation failed to give spectra with reproducible relative emission intensities. Furthermore, multiple emissions originating in π^* orbitals of different ligands cannot account for the emissions observed from $[\text{Ru}(\text{azpy})_3](\text{PF}_6)_2$, yet the emission spectrum of the latter is similar to that of the btz complex. Since $[\text{Ru}(\text{azpy})_2(\text{btz})](\text{ClO}_4)_2$ is a mixture of isomers and, although unresolved, geometric isomers of $\text{Ru}(\text{azpy})_3^{2+}$ are possible, we attribute the two emissions to different isomeric forms of the complexes even though the separation between the peaks indicates an isomer energy difference considerably larger than previously found.¹⁷

When $[\text{Ru}(\text{azpy})_3](\text{PF}_6)_2$ is dissolved in acetone, the 784- and 846-nm emissions are replaced by a single emission with a maximum at 835 nm. When the btz complex is dissolved in acetone, the 776- and 833-nm emissions disappear and the spectrum consists only of a short-wavelength tail of one or more emissions with maxima at ≥ 870 nm. These changes in the emission spectra are not due to a change in ligation about Ru(II). Although the entire spectrum is blue shifted, the relative energies and extinction coefficients of the near-UV-visible absorptions of $[\text{Ru}(\text{azpy})_3](\text{PF}_6)_2$, dispersed in a Nujol mull on a glass slide, are equivalent to those obtained from acetone solutions of the complex. If the hypothesis regarding isomers is correct, the occurrence of one emission may be due to a facile interconversion to one dominant isomeric form or only one isomer being luminescent in fluid solution.

In both the solid state and acetone solution, the Stokes shifts of the luminescence from these $\text{Ru}(\text{azpy})_2\text{L}_2^{n+}$ complexes exceed those found for luminescent $\text{Ru}(\text{bpy})_2\text{L}_2^{n+}$ complexes^{15,18-20} by ca. 2000 cm^{-1} . Significant enhancement of pyridine ring modes in the resonance Raman spectra of the bpy complexes indicates charge delocalization over a relatively large portion of the bpy ligand in the MLCT state. In contrast, the resonance Raman spectra of the azpy complexes show only weak enhancement of vibrations assignable to pyridine deformations and moderate enhancement for phenyl ring vibrations. The largest enhancement in the spectra of the azpy complexes is of the azo $\text{N}=\text{N}$ vibration and vibrations of bonds contiguous to the azo function. If the molecular distortions of the emissive MLCT state parallel those of the MLCT state populated on absorption, i.e., the state probed by the resonance Raman spectra, then in the luminescent state the transferred charge populates π^* orbitals in close proximity to the metal

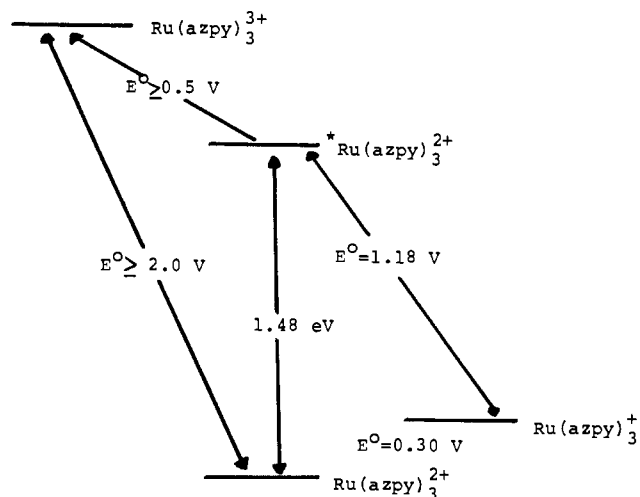


Figure 3. Ground- and excited-state redox potentials of $\text{Ru}(\text{azpy})_3^{2+}$ in aqueous solution at 25 °C (see text).

ion, principally localized on the azo function. This reduces the bond strength within this chromophore and, along with the increased flexibility of the azpy ligand, suggests that the azpy ligands accommodate the transferred charge by larger distortions of a more limited portion of the ligand.

Photoredox Properties and Emission Quenching. In fluid solution, the luminescent MLCT state of $\text{Ru}(\text{azpy})_3^{2+}$ lies 1.48 eV above the ground state. The MLCT states of the other $\text{Ru}(\text{azpy})_2\text{L}_2^{n+}$ complexes cannot be positioned exactly, although they must lie at ≤ 1.42 eV since the emission maxima occur at ≥ 870 nm. In past studies, the redox potentials of the MLCT state have been calculated from the difference in the excited-state energy and the thermal redox potentials of the ground state. Although the oxidation and reduction potentials of the $\text{Ru}(\text{azpy})_2\text{L}_2^{n+}$ complexes, listed in Table II, depend on the coligand, in general, the thermal redox chemistry, because of the π -accepting ability of the azpy ligand, is characterized by large oxidation and small reduction potentials. When compared to the MLCT state energy, these large differences in ground-state redox potentials yield an unusual energy level ordering, illustrated in Figure 3, in which the thermal redox potentials bracket the energy of the luminescent MLCT state. The emission spectra of the other $\text{Ru}(\text{azpy})_2\text{L}_2^{n+}$ complexes yield only upper limits of their LMCT-state energies, and therefore only limits of their excited-state potentials can be calculated. However, the limits listed in Table II suggest that, subject to slight changes in relative energies, Figure 3 is representative of all $\text{Ru}(\text{azpy})_2\text{L}_2^{n+}$ complexes.

In contrast to $\text{Ru}(\text{bpy})_3^{2+}$, where the MLCT state is essentially an equally exergonic oxidant or reductant, Figure 3 suggests that the LMCT state of $\text{Ru}(\text{azpy})_3^{2+}$ is an exergonic/oxidant and endergonic/reductant. As such, the complex offers a convenient test of the reliability of the luminescence-electrochemical cycles used to calculate excited-state redox potentials. Figure 3 suggests that, with a series of related redox partners, the reduced partner, R, will quench the MLCT state of $\text{Ru}(\text{azpy})_3^{2+}$, i.e.



provided the oxidation potential of R is -1.18 V. On the other hand, the oxidized partner, Ox, will quench, i.e.



only if its reduction potential and the $\text{Ru}(\text{azpy})_3^{2+}$ MLCT-state energy, 1.48 eV, exceed the ground-state oxidation potential of $\text{Ru}(\text{azpy})_3^{2+}$, ≥ 2.0 eV.

To test these conclusions, the quenching of $*\text{Ru}(\text{azpy})_3^{2+}$ by a series of reversible, one-electron redox couples, which

- (16) Sullivan, B. P.; Abruna, H.; Finklea, H. O.; Salmon, D. J.; Nagle, J. K.; Meyer, T. J.; Sprintschnik, H. *Chem. Phys. Lett.* **1978**, *58*, 389.
 (17) Krause, R. A.; Ballhausen, C. J. *Acta Chem. Scand., Ser. A* **1977**, *A31*, 535.
 (18) Demas, J. N.; Crosby, G. A. *J. Am. Chem. Soc.* **1971**, *93*, 2841.
 (19) Klassen, D. M. *Inorg. Chem.* **1976**, *15*, 3166.
 (20) Bock, C. R.; Meyer, T. J.; Whitten, D. G. *J. Am. Chem. Soc.* **1975**, *97*, 2909.

Table III. Stern–Volmer Constants and Bimolecular Rate Constants for Quenching of $\text{Ru}(\text{azpy})_3^{2+}$ in Aqueous Solution and the Standard Potentials for Oxidation or Reduction of the Quenchers

quencher	$K_{\text{sv}}, \text{M}^{-1}$	$k_{\text{b}},^a \text{M}^{-1} \text{s}^{-1}$	E°, V
MV^{2+}	10		-0.44
Fe^{2+}	1.5×10^4	3.6×10^{10}	-0.77
Fe^{3+}	10		+0.77
$\text{Fe}(\text{CN})_6^{4-}$	7.4×10^3	1.8×10^{10}	-0.36
$\text{Fe}(\text{CN})_6^{3-}$	10		+0.36
Ce^{3+}	10		-1.61
Ce^{4+}	1.5×10^3	3.6×10^9	+1.61

^a Calculated according to $K_{\text{sv}} = k_{\text{b}}t_0$, where $t_0 = 418 \text{ ns}$.

range in oxidation potential from -1.61 V ($\text{Ce}^{3+}/\text{Ce}^{4+}$) to +0.44 V ($\text{MV}^+/\text{MV}^{2+}$). MV^{2+} denotes the methylviologen dication) was measured. Comparing the absorption spectra of $\text{Ru}(\text{azpy})_3^{2+}$ in the presence and absence of the quenchers establishes that none undergo a reaction with ground-state $\text{Ru}(\text{azpy})_3^{2+}$. Quenching via energy transfer is discounted since the excited-state energies of the quenchers exceed that of $^*\text{Ru}(\text{azpy})_3^{2+}$ and, as described below, the observed quenching is consistent with the predicted energetics of photoinduced redox reactions.

The Stern–Volmer constants, K_{sv} , describing the quenching of $^*\text{Ru}(\text{azpy})_3^{2+}$ by the various quenchers are summarized in Table III. The data listed in Table III refer to measurements at room temperature ($22 \pm 1^\circ \text{C}$) in aerated 1.0 N H_2SO_4 solutions at an ionic strength of 1.5. The high acidity is necessary to prevent hydrolysis of the Fe^{2+} and Fe^{3+} species. In those cases where quenching occurs, plots of the relative emission intensity, I_0/I , measured at 830 nm, vs. $[\text{Q}]$ are linear through 90% quenching and corrections for trivial effects are $\leq 5\%$. The bimolecular quenching rate constants, k_{b} , listed in Table III are calculated from $K_{\text{sv}} = k_{\text{b}}t_0$, where t_0 is the luminescent lifetime of $^*\text{Ru}(\text{azpy})_3^{2+}$. The latter was measured under the same conditions as for the quenching experiments. Plots of the natural log of the emitted intensity vs. times are linear through 95% of the emitted light and yield a first-order emission decay rate constant of $(2.39 \pm 0.12) \times 10^6 \text{ s}^{-1}$ and a corresponding lifetime of $419 \pm 20 \text{ ns}$.

The Stern–Volmer constants and corresponding bimolecular rate constants listed in Table III corroborate the calculated energetics of photoredox quenching of $^*\text{Ru}(\text{azpy})_3^{2+}$. Oxidative quenching of the LMCT state by MV^{2+} is calculated to be endergonic by $\geq 0.7 \text{ eV}$, and consistent with the calculated energetics no quenching by MV^{2+} , $K_{\text{sv}} \leq 10 \text{ M}^{-1}$, occurs. The reduction potentials of $\text{Fe}(\text{CN})_6^{3-}$ and Fe^{3+} are 0.36 and 0.77 V, respectively. The absence of quenching by these species, $K_{\text{sv}} \leq 10 \text{ M}^{-1}$, suggests that oxidation of the MLCT state



is endergonic by $\geq 0.8 \text{ eV}$. Combining the latter value with the LMCT-state energy, 1.48 eV, yields $\geq 2.3 \text{ eV}$ for the oxidation potential of the ground-state $\text{Ru}(\text{azpy})_3^{2+}$, which is in reasonable agreement with the value of 2.2 V obtained by differential pulsed polarography.²¹ In view of the energetics of reaction 3, it is not surprising that the only species found to oxidatively quench $^*\text{Ru}(\text{azpy})_3^{2+}$ is the strong oxidant Ce^{4+} . The driving force for the reaction

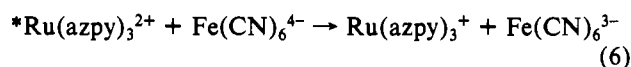


is ca. 0.9 eV, and quenching by Ce^{4+} occurs at essentially a diffusion-controlled rate, $k = 3.6 \times 10^9 \text{ M}^{-1} \text{ s}^{-1}$. Although reaction 4 has a favorable driving force, the $^*\text{Ru}(\text{azpy})_3^{2+}$ emission intensity in the presence of Ce^{4+} is not time dependent and absorption spectra recorded before and after the quenching experiments indicate no net chemical change. This suggests that concurrent with reaction 4 is an exergonic thermal back-reaction, $\Delta G \approx 0.6 \text{ eV}$, which regenerates $\text{Ru}(\text{azpy})_3^{2+}$ and Ce^{4+} .

In contrast to the endergonicity of reaction 3, reduction of the $\text{Ru}(\text{azpy})_3^{2+}$ LMCT state has a favorable driving force and reductive quenching by species whose oxidation potentials are $\geq -1.18 \text{ V}$ is energetically feasible. Since the oxidation potential of Ce^{3+} , -1.61 V, exceeds the latter value, reductive quenching by Ce^{3+} is not expected and, as indicated in Table III, no quenching, $K_{\text{sv}} \leq 10 \text{ M}^{-1}$, is detected. On the other hand, the reductive quenching reactions



and



have driving forces of +0.47 and +0.82 eV, respectively, and the data in Table III show that both species are facile quenchers. Neither quenching reaction leads to a spectrally detectable net chemical change since both are complimented by exergonic thermal back-reactions. The large bimolecular rate constant for quenching by $\text{Fe}(\text{CN})_6^{4-}$, $k_{\text{b}} = 1.8 \times 10^{10} \text{ M}^{-1} \text{ s}^{-1}$, seems reasonable in view of the electrostatic attraction between the species, but the value of $3.6 \times 10^{10} \text{ M}^{-1}$ for Fe^{2+} appears unusually large in spite of the additional driving force for a diffusion-controlled reaction between two dipoles. However, the ionic strength of the medium is high, $\mu = 1.5$, and Silverman and Dodson²³ point out that the self-exchange rate of the $\text{Fe}^{2+}/\text{Fe}^{3+}$ couple increases with increasing ionic strength.

The quenching rate listed in Table III are consistent with the calculated excited-state redox properties of $\text{Ru}(\text{azpy})_3^{2+}$. While the data do not establish the absolute redox potentials of the complex's MLCT state, it does attest, in the general sense, to the reliability of predictions based on electrochemical–luminescence cycles, which suffer from the philosophically bothersome point of comparing electrochemical potentials measured relative to the hydrogen couple and spectrally measured energy gaps. Furthermore, the unusual energy level ordering found for these $\text{Ru}(\text{azpy})_2\text{L}_2^{2+}$ complexes, where the thermal oxidation potential exceeds the energy of the luminescent MLCT state, suggests a unique inroad into chemiluminescent reactions of transition-metal complexes. That relatively few chemiluminescent reactions of $\text{Ru}(\text{bpy})_3^{3+}$ have been reported^{25,26} is not surprising since the reaction is both energetically and kinetically demanding. The electron-transfer reaction must not only be very rapid but the reductant must also be of sufficient potential to populate the $\text{Ru}(\text{bpy})_3^{2+}$ LMCT state, which lies 0.84 eV above the thermal oxidation potential of $\text{Ru}(\text{bpy})_3^{2+}$. As shown in Figure 3, however, the luminescent LMCT state of $\text{Ru}(\text{azpy})_3^{2+}$ is of lower energy than the thermal oxidation potential of the complex. Consequently, population of the LMCT state is, in principle, possible in the reduction of $\text{Ru}(\text{azpy})_3^{3+}$ by a very mild reductant. Unfortunately, our attempts to test this idea by generating $\text{Ru}(\text{azpy})_3^{3+}$ through reactions with strong oxidants

(21) Differential pulsed polarography unpublished results.
 (22) Based on Debye–Bronsted equations:

$$\log [k(\mu)] = \log [k(\mu = 0)] + 1.02Z_D Z_Q \mu^{1/2}$$

For more details see, e.g.: Glasstone, S. "Physical Chemistry", 2nd ed.; Macmillan: London, 1953; p 936.

(23) Silverman, J.; Dodson, R. W. *J. Phys. Chem.* **1952**, *56*, 846.

(24) Lyttle, F. E.; Hercules, D. M. *Photochem. Photobiol.* **1971**, *13*, 123.

(25) Martin, J. E.; Hart, E. J.; Adamson, A. W.; Gafney, H. D.; Halpern, J. *J. Am. Chem. Soc.* **1972**, *94*, 9238.

(26) Rubenstein, I.; Bard, A. J. *J. Am. Chem. Soc.* **1981**, *103*, 512.

were unsuccessful. Syntheses of new π -accepting ligands which will form Ru(II) complexes that are easier to oxidize but at the same time retain the unusual energy level ordering illustrated in Figure 3 are in progress.

Acknowledgment. H.D.G. thanks the Andrew W. Mellon Foundation for a fellowship during 1981-1982. Financial support of this research by the Research Foundation of the City University of New York, the Dow Chemical Co. Technology Acquisition Program, and the donors of the Petroleum

Research Fund, administered by the American Chemical Society, is gratefully acknowledged.

Registry No. Ru(azpy)₂(CN)₂, 80697-52-5; Ru(azpy)₂(NO₂)₂, 80697-51-4; Ru(azpy)₂(btz)²⁺, 80697-57-0; Ru(azpy)₂(bpy)²⁺, 80697-55-8; Ru(azpy)₃²⁺, 80697-53-6; Ru(azpy)₂(en)²⁺, 80697-59-2; Ru(azpy)₂(acac)⁺, 80697-64-9; Ru(azpy)₂Br₂, 80735-95-1; Ru(azpy)₂(N₃)₂, 80697-61-6; Ru(azpy)₂Cl₂, 80735-96-2; Ru(azpy)₂(tu)₂²⁺, 80697-62-7; Fe(CN)₆⁴⁻, 13408-63-4; Fe(CN)₆³⁻, 13408-62-3; Fe²⁺, 15438-31-0; Fe³⁺, 20074-52-6; Ce³⁺, 18923-26-7; Ce⁴⁺, 16065-90-0.

Contribution from the Research School of Chemistry,
The Australian National University, Canberra, ACT 2601, Australia

Stereochemistry and Dynamic Properties of Square-Planar and Square-Pyramidal Cations of Bivalent Nickel, Palladium, and Platinum Containing the Enantiomers of (*R**,*R**)-(±)- and (*R**,*S**)-(±)-1-(Methylphenylarsino)-2-(methylphenylphosphino)benzene

GEOFFREY SALEM and STANLEY BRUCE WILD*

Received September 9, 1983

Square-planar and square-pyramidal complexes of bivalent nickel, palladium, and platinum containing the enantiomers of (*R**,*R**)-(±)- and (*R**,*S**)-(±)-1-(methylphenylarsino)-2-(methylphenylphosphino)benzene (phas) have been prepared, and their behavior in solution has been investigated by ¹H and ³¹P NMR spectroscopy. All possible stereoisomers of the different species have been detected and unambiguously identified. The kinetically stable complex (+)-[Ni([*R**,*S**)]-phas)₂](ClO₄)₂ is stereochemically nonrigid at 304 K in MeCN-*d*₃. The corresponding five-coordinate chloro species are also nonrigid but exhibit facile redistribution of the bidentates under ambient conditions. In the absence of free ligand the compounds [MCl(phas)₂]Cl (where M = Pd and Pt) are kinetically stable with respect to redistribution of the bidentate ligands but undergo intramolecular cis-trans isomerization upon heating. Reaction of (*R**,*R**)-(±)-phas with (±)-[MCl₂(*R**,*R**)-phas] produces crystalline meso complexes only, although the corresponding racemic complexes are of comparable stability. The square-planar cations are more stable: the complexes [Pt(phas)₂](PF₆)₂ do not undergo redistribution of bidentates in the presence of free ligand under ambient conditions.

Introduction

Although numerous unsymmetrically substituted bis(tertiary) ligands containing phosphorus and arsenic are known,¹ the stereochemistry and dynamic properties of their metal chelates have been little explored. Chiral molecules of this type are of considerable interest in connection with the development of inorganic systems for asymmetric synthesis, since they are capable of exercising an electronic, as well as steric, control over the site of attack of a reactant on a coordinated prochiral substrate. The present work is concerned with the behavior of bivalent complexes of nickel, palladium, and platinum containing the enantiomers of the unsymmetrical bidentate (*R**,*R**)-(±)- and (*R**,*S**)-(±)-1-(methylphenylarsino)-2-(methylphenylphosphino)benzene (phas). The resolution of both diastereoisomers of this ligand has recently been achieved by the method of metal complexation.² The four enantiomers of the ligand are depicted in Figure 1.^{3,4} The work is complementary to our earlier studies of tetrahedral gold(I) complexes⁵ of this ligand, as well as of the symmetrical donor equivalents 1,2-phenylenebis(methylphenylphosphino)⁶ and its arsenic analogue,⁷ for which the bivalent nickel,⁸

palladium, and platinum⁹ chemistry has already been described.

Results and Discussion

Preparations. (a) Nickel(II) Complexes. The square-planar complexes [Ni(phas)₂](ClO₄)₂ were obtained in high yield from the reaction of [Ni(H₂O)₆](ClO₄)₂ with the appropriate form of the ligand in acetone. The salts are orange diamagnetic solids that conduct as di-univalent electrolytes in acetonitrile solution. The corresponding deep-red to purple compounds [NiCl(phas)₂]ClO₄ were derived from the square-planar species by the addition of chloride. Conductivity and spectroscopic data are consistent with the assignment of a five-coordinate square-pyramidal geometry to the cationic chloride adducts. Selected physical and spectroscopic data for the various stereoisomeric forms of the compounds [Ni(phas)₂](ClO₄)₂ and [NiCl(phas)₂]ClO₄ are presented in Table I.

(b) Palladium(II) and Platinum(II) Complexes. The optically active square-planar complexes [PdCl₂L] (where L = [*R*-(*R**,*R**)]-, [*S*-(*R**,*R**)]-, [*R*-(*R**,*S**)]-, or [*S*-(*R**,*S**)]-phas) were obtained as described in the resolution procedure.² The corresponding racemic compounds were prepared from the appropriate form of the ligand and [PdCl₂(MeCN)₂] in boiling acetonitrile. Platinum analogues were produced by hydrochloric acid treatment of the cations resulting from

(1) McAuliffe, C. A.; Levason, W. "Phosphine, Arsine and Stibine Complexes of Transition Metals"; Elsevier: New York, 1979; p 16.

(2) Salem, G.; Wild, S. B. *Inorg. Chem.* **1983**, *22*, 4049.

(3) The nomenclature used through this paper is consistent with that used by the Chemical Abstracts Service.⁴ In the present situation [*R*-(*R**,*S**)]-phas denotes *R*-As,*S*-P.

(4) Sloan, T. E. *Top. Stereochem.* **1981**, *12*, 1.

(5) Palmer, J. A. L.; Wild, S. B. *Inorg. Chem.* **1983**, *22*, 4054.

(6) Roberts, N. K.; Wild, S. B. *J. Am. Chem. Soc.* **1979**, *101*, 6254.

(7) Roberts, N. K.; Wild, S. B. *J. Chem. Soc., Dalton Trans.* **1979**, 2015.

(8) Roberts, N. K.; Wild, S. B. *Inorg. Chem.* **1981**, *20*, 1892.

(9) Roberts, N. K.; Wild, S. B. *Inorg. Chem.* **1981**, *20*, 1900.